

# Journal of Geophysical Research: Atmospheres

## RESEARCH ARTICLE

10.1002/2015JD023119

**Key Points:**

- We found strong 5 day PWs in polar winter and secondary peak in summer mesopause
- W1 5 day PW in temperature is almost anticorrelated with that in IWC of PMCs
- Phase shift of W1 5 day PW in T and IWC of PMCs is 2.0 (0.3) h in NPR (SPR)

**Correspondence to:**X. Liu,  
xliu@spaceweather.ac.cn**Citation:**

Liu, X., J. Yue, J. Xu, W. Yuan, J. M. Russell III, and M. E. Hervig (2015), Five-day waves in polar stratosphere and mesosphere temperature and mesospheric ice water measured by SOFIE/AIM, *J. Geophys. Res. Atmos.*, 120, 3872–3887, doi:10.1002/2015JD023119.

Received 15 JAN 2015

Accepted 10 APR 2015

Accepted article online 16 APR 2015

Published online 11 MAY 2015

## Five-day waves in polar stratosphere and mesosphere temperature and mesospheric ice water measured by SOFIE/AIM

**Xiao Liu<sup>1,2</sup>, Jia Yue<sup>3</sup>, Jiayao Xu<sup>2</sup>, Wei Yuan<sup>2</sup>, James M. Russell III<sup>3</sup>, and Mark E. Hervig<sup>4</sup>**

<sup>1</sup>College of Mathematics and Information Science, Henan Normal University, Xinxiang, China, <sup>2</sup>State Key Laboratory of Space Weather, Center for Space Science and Applied Research, Chinese Academy of Sciences, Beijing, China, <sup>3</sup>Atmospheric and Planetary Sciences, Hampton University, Hampton, Virginia, USA, <sup>4</sup>GATS, Inc., Driggs, Idaho, USA

**Abstract** The temperature and column ice water content (IWC) of polar mesospheric clouds (PMCs) have been simultaneously measured by the Solar Occultation for Ice Experiment (SOFIE) on board NASA's Aeronomy of Ice in the Mesosphere satellite since April 2007. The 8 year (2007–2014) data of the temperature and IWC are used to extract the 5 day planetary waves (PWs) with zonal wave numbers ranging from –1 to –3 (eastward propagating mode, E1–E3), 0 (stationary mode, W0), and 1 to 3 (westward propagating mode, W1–W3) in the polar stratosphere and mesosphere. The 5 day PWs in temperature are stronger in the polar winter stratosphere and mesosphere and exhibit substantial interhemispheric asymmetry. The date-height distributions of the 5 day waves coincide with those of the eastward jet in each hemisphere. This indicates that the 5 day PWs might be generated from barotropic/baroclinic instability in the polar stratosphere. The relative strengths of 5 day PWs decrease with increasing wave numbers. The E1 (W1) 5 day PW is stronger than any other mode in the winter stratosphere and lower mesosphere (summer upper mesosphere). SOFIE temperature and IWC data are derived from simultaneous measurements in the same air column and thus provide a good opportunity to study the phase relationship between the 5 day PWs in temperature and IWC. Our analyses show that the phase shifts of W1 5 day PW in temperature relative to that in IWC have a mean of –2.0 h (0.3 h) with a standard deviation of 3.8 h (4.2 h) in the northern (southern) polar region. This indicates that the formation of the W1 5 day PW in PMCs is controlled mainly by the W1 5 day PW in temperature and influenced by other factors and is consistent with previous studies.

### 1. Introduction

Planetary waves (PWs) are the large-scale disturbances resulting from the longitudinal variations in topography and heating and are balanced by the Coriolis force. The normal modes of traveling PWs have periods of 2 days, 5 days, 10 days, and 16 days [Charney and Drazin, 1961; Madden, 1979; Kasahara, 1976; Salby, 1981; Forbes, 1995]. Both numerical simulations and observations have revealed that PWs play important roles in atmospheric dynamics and ionospheric electrodynamics [Altadill and Apostolov, 2003; Pogoreltsev et al., 2007; Jiang et al., 2008; Liu et al., 2010; Yue et al., 2012].

Ground-based network observations provide the opportunity to characterize PW periods, phases, and zonal wave numbers [Kovalam et al., 1999; Luo et al., 2002; Jiang et al., 2008]. Compared with ground-based observations, satellite observations have their advantage in offering the opportunity to study the global structure of PWs. Our understanding of the global structure of PWs has advanced greatly from the observations from the Sounding of the Atmosphere using Broadband Emission Radiometry (SABER) instrument on board the Thermosphere Ionosphere Mesosphere Energetics and Dynamics satellite and from both the High Resolution Doppler Imager and Wind Imaging Interferometer on board the Upper Atmosphere Research Satellite [Wu et al., 1994; Clark et al., 2002; Garcia et al., 2005; Riggin et al., 2006; Pancheva et al., 2010; Pancheva and Mukhtarov, 2011, and references therein; Shepherd et al., 2012].

Polar Mesospheric Clouds (PMCs) are a thin layer of ice particles at the polar summer mesopause. The formation of PMCs is dependent on the cumulative effects of water vapor, low temperature, and nucleation nuclei. The occurrence and strength of PMCs are highly related to the dynamics and microphysics of the polar summer mesosphere and are thus a sensitive indicator of global temperature and water vapor changes [Thomas, 1996; Hervig et al., 2001, 2009a, 2009b, 2013; Rapp and Thomas, 2006]. Using 40 years PMC data from a network

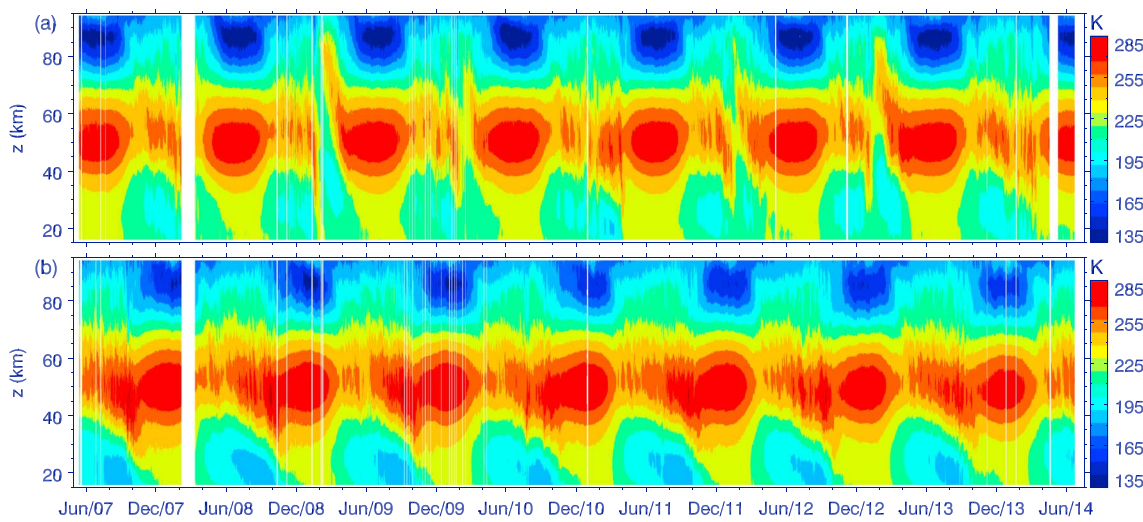


**Figure 1.** Daily averaged temperature from the SOFIE observation in the (a) NPR and (b) SPR from 2007 to 2014. The missing data are indicated as white gaps. The date (month/year) denotes the first of each calendar month.

observation in Europe, Kirkwood and Stebel [2003] found a strong correlation between the occurrence of PMC and PWs in the PMC height. Then studies have revealed the 5 day PW in PMC brightness measured from the Student Nitric Oxide Explorer (SNOE) satellite [Merkel et al., 2003]. Subsequently, using PMC data from the Scanning Imaging Absorption spectrometer for Atmospheric CHartographY on board the European Space Agency's Envisat spacecraft and the temperature data measured by Microwave Limb Sounder (MLS) on board NASA's Earth Observing System Aura satellite, von Savigny et al. [2007] have shown a good agreement in the 5 day PW of PMC occurrence rates and mesopause temperature. By studying the PMC brightness measured by SNOE and the temperature measured by the SABER instrument, Merkel et al. [2008] found that the 5 day PW in the PMC brightness and temperature are almost anticorrelated.

Further studies on the 5 day PW in temperature and PMC were performed following the launch of NASA's Aeronomy of Ice in the Mesosphere (AIM) satellite on 25 April 2007 [Benze et al., 2009; Merkel et al., 2009; Nielsen et al., 2010]. Benze et al. [2009] have identified a 5 day wave in early August both in the PMC occurrences measured by the Cloud Imaging and Particle Size (CIPS) instrument on board AIM and by the second generation Solar Backscatter Ultraviolet satellite instruments. Using the coincident observations of PMC brightness from the CIPS instrument and temperature from SABER instrument in the 2007 northern summer, Merkel et al. [2009] found that the 5 day PW with westward wave number 1 (W1) was presented in both PMC brightness and temperature.

Although the W1 5 day PWs in PMC brightness and temperature are almost anticorrelated, Merkel et al. [2008, 2009] showed that the PMC brightness maximum occurs 10 h before the temperature minimum. Subsequently, using the CIPS PMC data, Solar Occultation for Ice Experiment (SOFIE) PMC data, and Navy Operational Global Atmospheric Prediction System–Advanced-Level Physics High-Altitude temperature, Nielsen et al. [2010] also found the 10 h phase shift between PMC brightness and temperature when the W1 5 day PW is strongest during August 2007. Here we note that these measurements (SNOE, SABER, CIPS, and SOFIE) are most likely not in the same air column even though the measurement time might be concurrent within some reasonable interval. Moreover, SABER temperature observations in polar summer cover only approximately 20 days before and after the solstice due to the spacecraft yaw. Thus, it cannot provide the temperature information over the entire PMC season. The phase shift of the W1 5 day PW in PMC and temperature should therefore be further examined using the simultaneous measurements of temperature and the PMC vertical column ice water content (IWC) over the entire PMC season using the SOFIE instrument on board the AIM satellite.

One focus of this paper is to study the climatologies of 5 day PWs in the polar stratosphere and mesosphere from the continuous temperature observations from the SOFIE instrument. Since the SOFIE-derived IWC is used to characterize PMCs [Hervig et al., 2001, 2009a, 2009b, 2013], another objective is to study the phase relationship of the W1 5 day PW in temperature and IWC.

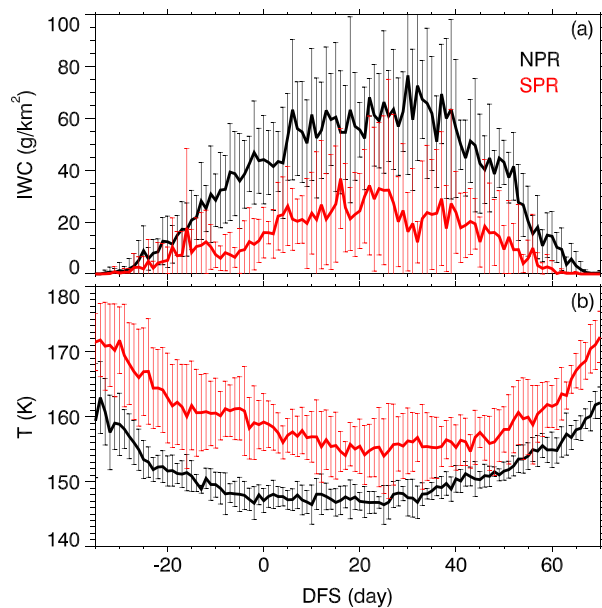


**Figure 2.** A composite daily averaged (a) IWC and (b) temperature in the summer NPR (black) and SPR (red) from 2007 to 2014. The temperature was first averaged over the altitude range of 81 to 87 km before the daily average was performed. The DFS labeled below the x axis is the day numbers from summer solstice (21 June in the NPR and 21 December in the SPR).

The remainder of this paper is organized into four sections. Section 2 describes the data and PW extraction method. Section 3 presents the seasonal variations and interhemispheric asymmetry of the climatologies of 5 day PWs, as well as their height and wave number dependence. Section 4 analyzes the phase shift of the W1 5 day PWs in temperature and IWC, and section 5 presents our summary and conclusions. The significant test, which is important for the analysis results, is given in the Appendix A.

## 2. Data and Analysis Method

### 2.1. Data

The AIM satellite is in a nearly circular, sun-synchronous retrograde orbit with an inclination of 97.4°, with the aim of studying the dynamics and formation of PMCs. A detailed description of the AIM satellite can be found in *Russell et al.* [2009]. The SOFIE instrument on board the AIM satellite has measured temperature profiles in the height range from 10 to 102 km with a vertical resolution of 1 to 2 km and IWC in the Arctic and Antarctic since May 2007. A detailed description of SOFIE measurements and validation results can be found in *Gordley et al.* [2009], *Hervig et al.* [2009a, 2009b, 2013], *Marshall et al.* [2011], and *Stevens et al.* [2012]. The measurement local time transits from around 13:30 local solar time (LST) in the winter months to around 23:30 LST in the summer months of the northern polar region (NPR) and transits from around 10:30 LST in the winter months to around 1:30 LST in the summer months of the southern polar region (SPR). The temperature profile and IWC are taken at 15 longitudes and at the same local time each day. The latitude coverage of the SOFIE measurements ranges from approximately 65° to 86° north or south [*Hervig et al.*, 2013].

In this study, each SOFIE temperature profile was averaged vertically over 2 km before the PWs were extracted. We show in Figure 1 the daily averaged temperature as a function of date and height from 2007 to 2014. Prominent features in Figure 1 are the sudden stratospheric warming (SSW) events in January of 2009, 2010, 2012, and 2013 in the NPR. A detailed description of the SSW events observed by the SOFIE instrument can be found in *Thurairajah et al.* [2014] and *Bailey et al.* [2014]. By contrast, there is no SSW event in the SPR during AIM operation. Thus, the temperature structure is more stable in the SPR than in the NPR.

The daily averaged IWC (black line) shown in Figure 2 illustrates that the IWC appears mainly in June, July, and August in the NPR and in December, January, and February in the SPR. These occur mainly in the time interval from –30 to 60 days from summer solstice (DFS), which is 21 June in the NPR and 21 December in the SPR. Figure 2 shows that the IWC in the NPR is greater than that in the SPR and persists for a longer

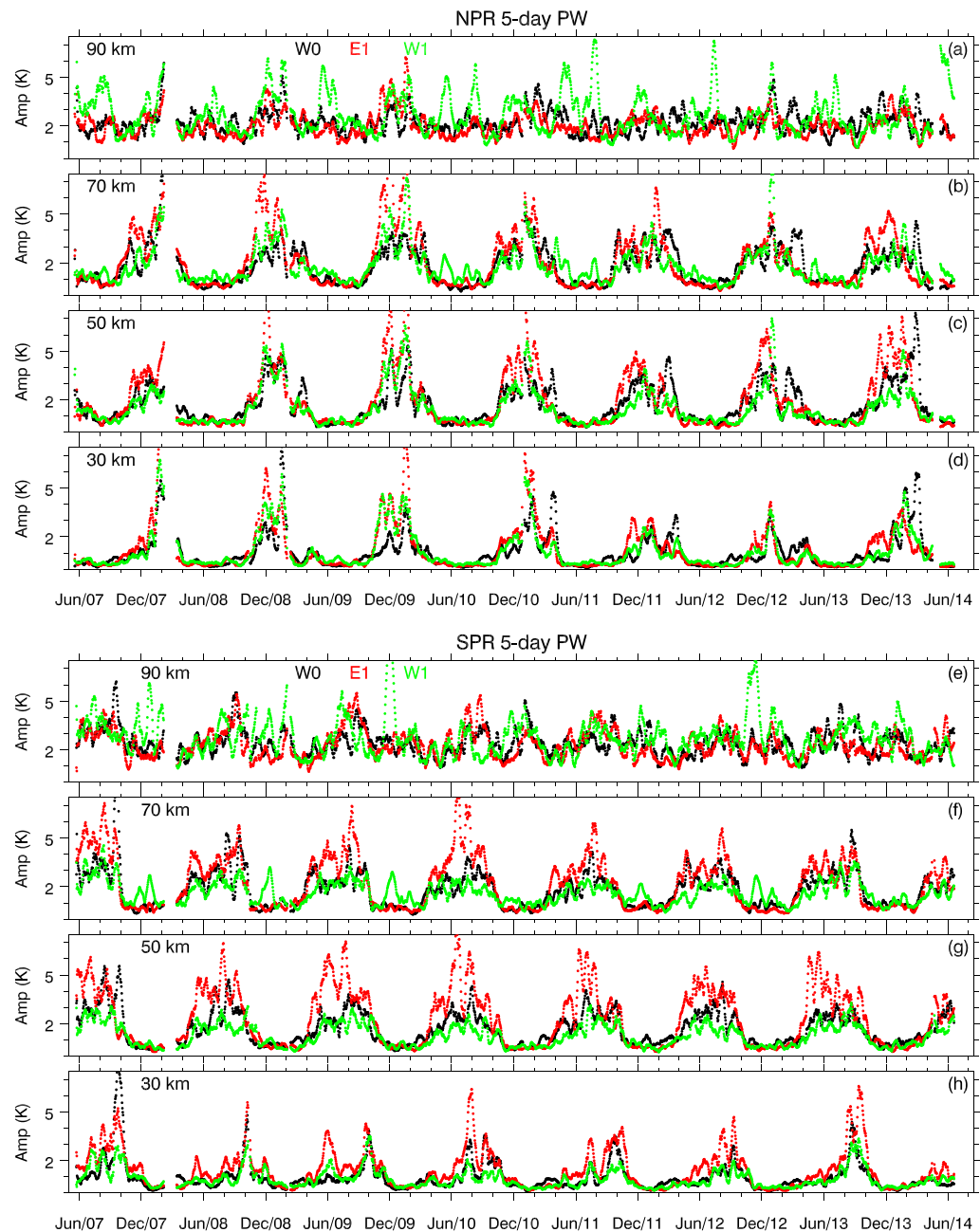


**Figure 3.** Amplitudes of 5 day PWs with zonal wave numbers of 0 (W0, black),  $-1$  (eastward, E1, red), and  $1$  (westward, W1, green) at the heights of (a and e)  $90$  km, (b and f)  $70$  km, (c and g)  $50$  km, and (d and h)  $30$  km derived from SOFIE temperature observations in the (Figures 3a–3d) NPR and (Figures 3e–3h) SPR from  $2007$  to  $2014$ . The date (month/year) denotes the first of each calendar month.

time [Hervig *et al.*, 2013]. The statistical study by Hervig *et al.* [2013] has shown that the ice layer is located mainly at the altitude range of  $81$  to  $87$  km in both the NPR and SPR. Thus, we show in Figure 2 the daily averaged temperature between  $81$  and  $87$  km (red line). Figure 2 shows that the IWC is greater when the temperature is lower. It should be noted that the IWC appeared in the SPR when the temperature were not cold enough (e.g.,  $160$  K in the SPR). This is because the warm bias of temperature in the SPR is larger than that in the NPR by  $5$  K in the mesopause [Hervig *et al.*, 2013]. We note that both the temperature profiles and IWC are measured simultaneously. Thus, the phase shift between the W1 5 day PWs in temperature and PMC can be examined accurately.

## 2.2. Analysis Method

In this work, 5 day PWs with zonal wave numbers of  $-3$  to  $3$  are extracted by performing a least squares (LS) fitting simultaneously on space-time series of temperature profiles and IWC, respectively. This method was designed by *Wu et al.* [1995] to study the unevenly sampled data of satellite observations. The negative (positive) wave numbers indicate the eastward (westward) propagating PWs. A brief description of this method is as follows.

The observational data  $y_i$  at time  $t_i$  (units in UT day) and longitude  $\lambda_i$  (normalized by  $2\pi$ , units in rad) are fitted by the following equation:

$$y_i = A \cos(\sigma t_i + s\lambda_i - \varphi). \quad (1)$$

Here  $A$  and  $\varphi$  are the amplitude and phase of the space-time series, respectively. For the westward moving sun-synchronous orbit of the AIM satellite, the relations between the longitude  $\lambda_i$  and UT can be expressed simply as  $\lambda_i = 2\pi t_i / (1 \text{ day})$ . The frequency (in cycles per day) and zonal wave number are  $\sigma = 2\pi / (l \text{ day})$  and  $s$ , respectively. Here  $l$  is the period of PW to be fitted. Thus, we have

$$y_i = A \cos\left[2\pi\left(\frac{1}{l} - s\right)t_i - \varphi\right]. \quad (2)$$

Equation (2) can be solved using the LS method developed by *Lomb* [1976].

The confidence level (CL) must be provided to assess the credibility of the extracted PWs. In this study, the Monte Carlo method is used to calculate the confidence level of PWs in each fitting window [*Pardo-Igúzquiza and Rodríguez-Tovar*, 2012]. After testing, we choose a 5 day window for the following analysis and slide the window forward 1 day to get the time series of 5 day PWs, as outlined in the Appendix.

## 3. Climatologies of 5 day PWs in the NPR and SPR

### 3.1. Seasonal Variations

To describe the seasonal variations of 5 day PWs, we first define the four seasons. The spring (autumn) months are March, April, and May in the NPR (SPR). The summer (winter) months are June, July, and August in the NPR (SPR). The autumn (spring) months are September, October, and November in the NPR (SPR). The winter (summer) months are December, January, and February in the NPR (SPR).

Figure 3 shows the amplitudes of 5 day PWs of W0, E1, and W1 derived from SOFIE temperature observations at three heights in the NPR and SPR from 2007 to 2014. It can be seen that these 5 day PWs are stronger in winter than in the other three seasons in the stratosphere (e.g., 30 km (Figures 3d and 3h) and 50 km (Figures 3c and 3g)) and middle mesosphere (e.g., 70 km (Figures 3b and 3f)) in both hemispheres. However, in the upper mesosphere (e.g., 90 km (Figures 3a and 3e)), the amplitudes of 5 day PWs in winter and summer are comparable. Moreover, the W1 5 day PWs (shown as a green line) are sometimes stronger in later spring and summer.

The 5 day PWs in the stratosphere and lower mesosphere are stronger in winter than those in summer. The E1 mode is stronger than the W0 and W1 modes in the winter stratosphere and lower mesosphere of both NPR and SPR. The stronger PWs with periods of 1 to 5 days are special phenomena in the winter polar stratosphere [*Manney and Randel*, 1993; *Allen et al.*, 1997; *Coy et al.*, 2003; *Watanabe et al.*, 2009; *Lu et al.*, 2013]. By analyzing the temperature from Modern Era Retrospective-Analysis for Research and Applications (MERRA) data, *Lu et al.* [2013] showed that the 1 to 5 day PWs are confined to the polar region with latitudes higher than  $45^\circ\text{S}$ . They concluded that the stronger 1 to 5 day PWs in the winter polar region are generated from barotropic/baroclinic instability in the polar night jet and/or double-jet structure in the winter polar stratosphere. This can explain the stronger 5 day PWs in the winter stratosphere shown here, which will be further discussed in section 3.3.

The seasonal variation of the W1 5 day PWs in the mesosphere is similar to that observed by meteor radars at Esrange ( $68^\circ\text{N}, 21^\circ\text{E}$ ) in the Arctic and Rothera ( $68^\circ\text{S}, 68^\circ\text{W}$ ) in the Antarctic, respectively. These ground-based studies showed that 5 day PWs are stronger in winter and later summer in the height range of 80 to 100 km. The summer 5 day PWs occurred mostly at a higher height with a peak around 95 km [*Pancheva and Mitchell*, 2004; *Day and Mitchell*, 2010]. The westward 5 day PWs should be blocked by the strong westward wind in

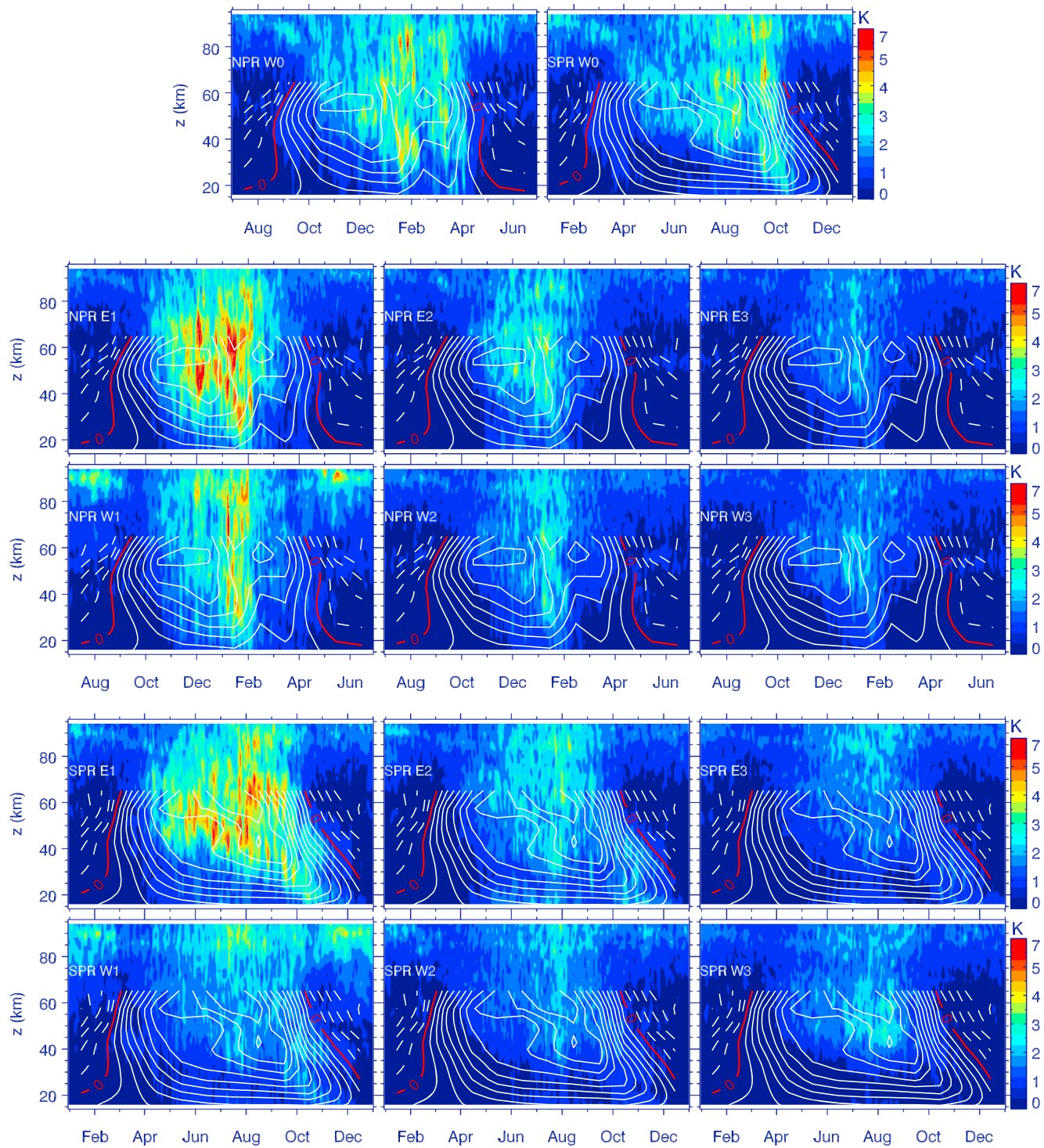


**Figure 4.** A composite year analysis of the amplitudes of 5 day PWs of W0–W3 and E1–E3 in the NPR and SPR for the years 2007–2014. The contour lines are the corresponding composite of zonal mean zonal winds calculated from the Modern Era Retrospective-Analysis for Research and Applications (MERRA) data in the same time period of SOFIE observations. The red solid, white dashed, and white solid contour lines indicate the zero wind, westward wind, and eastward wind, respectively. The interval of each contour line is  $5 \text{ ms}^{-1}$ . To compare the 5 day PWs in the NPR and SPR conveniently, we shift the date forward 6 months in the NPR. The date denotes the first of each calendar month.

the stratosphere and mesosphere during summer and cannot propagate into the mesosphere and lower thermosphere (MLT) region directly from the lower atmosphere [Charney and Drazin, 1961]. Therefore, the observed summertime 5 day PWs should come from other sources. The strong summertime 5 day PWs may be generated in the winter hemisphere and be ducted across the equator into the summer hemisphere. They may also be generated *in situ* by baroclinic instability in the MLT region [Riggin et al., 2006; Nielsen et al., 2010].

The seasonal variations of the W1 5 day PW are different from those of the W1 6.5 day PW, which has maxima before and after the equinoxes and is minimized at solstices [Liu et al., 2004]. The 6.5 day PW is not likely a result of a Doppler shift of the 5 day wave. Both might be generated from baroclinic/barotropic instability [Lieberman et al., 2003; Liu et al., 2004; Lu et al., 2013]. Moreover, the 5 day waves occur in the polar region and the 6.5 day wave in the low and middle latitudes [Wu et al., 1994; Lawrence and Randel, 1996; Riggin et al., 2006].

### 3.2. Wave Number and Height Dependence

To show the wave number and height dependence of 5 day waves, we combine the SOFIE results into 1 year with respect to the day numbers of each year, shown in Figure 4. We overplot in Figure 4 the zonal mean zonal winds (contour lines) calculated from the monthly mean MERRA data in the same time period. Figure 4 shows that both the stationary mode (W0; Figure 4, first row) and propagating modes (E1–E3 and W1–W3) of 5 day PWs occur mainly in the wintertime stratosphere and mesosphere. They are weak in the summer mesosphere, with the exception of the W1 mode in both the NPR and SPR.

It has been discussed that the eastward propagating PWs might be a special phenomenon in the winter polar stratosphere and extend to the mesosphere (Figure 4, second and fourth rows). These PWs are generated from baroclinic/barotropic instability in the polar night jet and/or double-jet regions [Garcia et al., 2005; Palo et al., 2005; Lu et al., 2013]. The strongest W1 mode is the gravest symmetric Rossby mode of 5 day PWs, the theory and observations of which have been studied extensively [Salby, 1981; Prata, 1989; Wu et al., 1994; Riggin et al., 2006; Pancheva et al., 2010; Pancheva and Mukhtarov, 2011]. It should be noted that these studies focused on E1 and/or W1 5 day PWs. Detailed analyses on the 5 day PWs with higher wave numbers are absent in the polar stratosphere and mesosphere. From Figure 4, we find that among the three eastward propagating modes (Figure 4, second and fourth rows), E1 is the strongest one and E2 is generally stronger than E3 in both the NPR and SPR. The strongest E1 mode is consistent with the 4 to 5 day PWs derived from the MERRA data [Lu et al., 2013]. Among the three westward propagating modes (Figure 4, third and fifth rows), W1 is the strongest in both the NPR and SPR and W2 is stronger (weaker) than W3 in the NPR (SPR).

Figures 4 illustrates that the seasonal variations of 5 day PWs are dependent on height and zonal wave numbers. The W1 5 day PW in the upper mesosphere is maximized in summer and winter. By contrast, it is minimized during March–April and September–October in the NPR and during March–April and October in the SPR. This induces the semiannual variation of the W1 5 day PW. The 5 day PWs of other modes (W0, W2, W3, and E1–E3) in the upper mesosphere also exhibit similar but weaker semiannual variation. This can account for the weak amplitudes of these modes (W0, W2, W3, and E1–E3) during summer and autumn in the upper mesosphere. All these 5 day PWs have peaks in the wintertime and exhibit strong annual variations in the stratosphere and lower mesosphere.

### 3.3. Interhemispheric Asymmetry and Height Dependence

From Figure 4, we can see that the 5 day PWs are asymmetric between the two hemispheres. Moreover, this interhemispheric asymmetry is dependent on height and zonal wave numbers. The W0 5 day PWs have similar magnitude but different date-height distributions in the NPR and SPR. In the stratosphere, the W0 5 day PW is stronger in the NPR than in the SPR in winter.

The 5 day PWs of E1–E3 and W1–W3 in the stratosphere and lower mesosphere exhibit substantial interhemispheric asymmetry, which varies in height (Figure 4). In the upper stratosphere and lower mesosphere, the 5 day PWs of E1–E3 and W1–W3 become prominent (amplitude  $\geq 2$  K) at almost the same time, in October (NPR) and April (SPR). However, they disappear (amplitude  $< 2$  K) at different times, indicating a dependence on height. In the lower mesosphere, the 5 day PWs of E1–E3 and W1–W3 disappear in early March in the NPR, which is 1 month earlier than those in early October in the SPR. In the

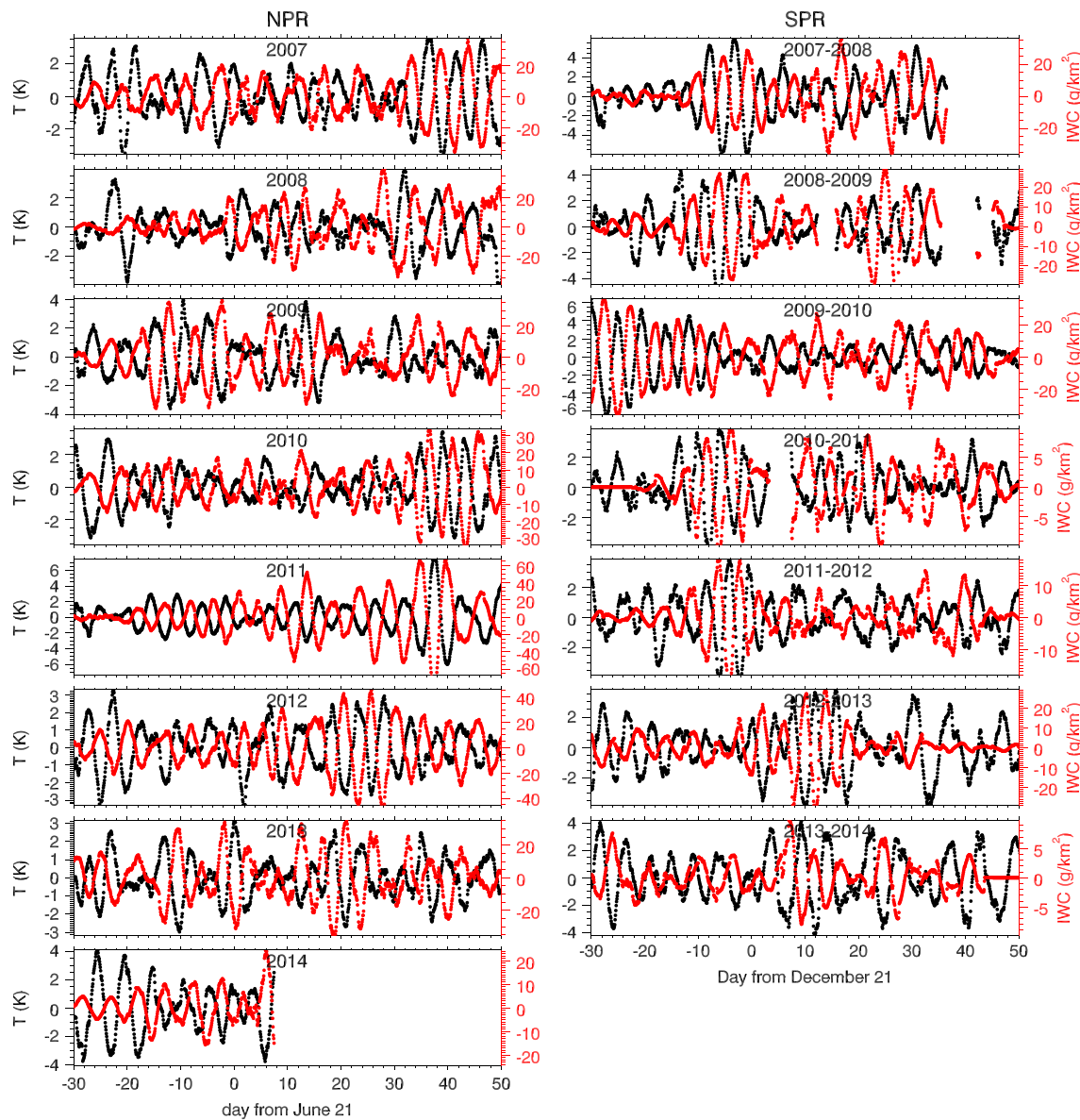


**Figure 5.** Temporal evolution of W1 5 day PWs in temperature averaged over the height range of 81 to 87 km (black, left axis) and IWC (red, right axis) at 120°E during the summers of (left) NPR and (right) SPR from 2007 to 2014. The x axis labels the DFS (days from summer solstices 21 June in the NPR and 21 December in the SPR). The years are labeled in each panel.

upper stratosphere, the 5 day PWs of E1–E3 and W1–W3 also disappear in early March in the NPR, which is far earlier (almost 2 months) than late October in the SPR. In the lower stratosphere, the 5 day PWs of E1–E3 and W1–W3 become prominent also simultaneously in November and disappear in late February in the NPR. However, in the SPR, the 5 day PWs of E1–E3 and W1 exhibit an apparent phase shift from May at about 40 km to early November at about 20 km. For the 5 day PWs of W2 and W3, they are very weak in the lower stratosphere in the SPR.

We find that the 5 day PWs extend to a later time and lower altitude in the SPR than in the NPR (Figure 4). Interestingly, the MERRA zonal wind data in the SPR (contour lines in Figure 4) have shown that the peak of eastward zonal wind extends to a later time and lower altitude in the SPR. The polar night jet and/or double-jet structure and the corresponding baroclinic/barotropic instabilities in the southern hemisphere have been revealed in the MERRA data by *Lu et al.* [2013]. By analyzing the Eliassen-Palm flux divergence, they conclude that stratospheric polar night jet and/or the double-jet structure is the source of PWs. Thus,

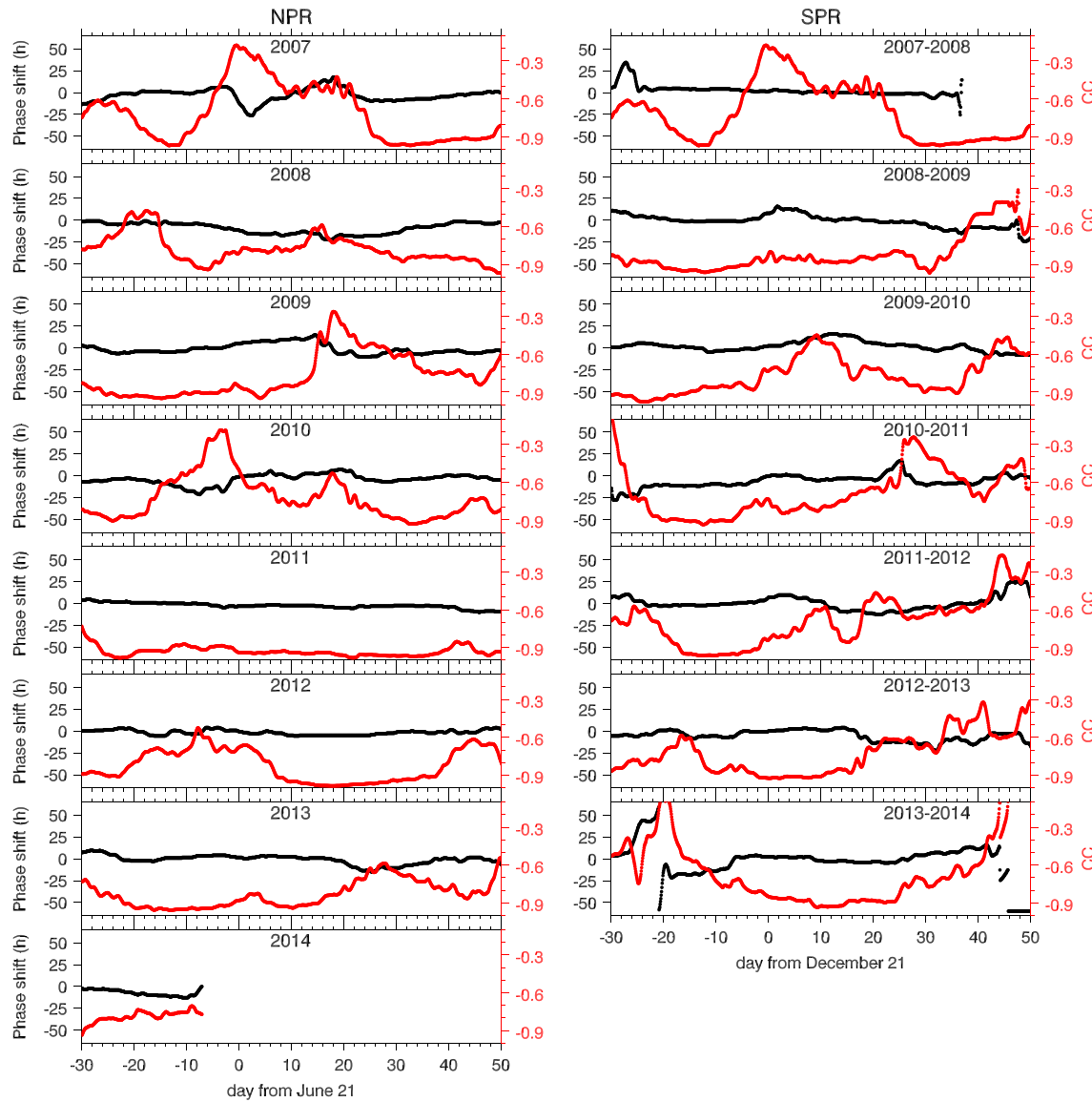


**Figure 6.** Temporal evolution of the phase shift (black, left axis) when the correlation coefficient (CC) is minimized. The minimum CC means that the minimum CC is achieved after varying the phase shift of W1 5 day PWs in temperature and IWC within a window of 15 days. Then we move the window forward by 1/15 day to get the time series of minimum CC during the summers of (left) NPR and (right) SPR from 2007 to 2014. The phase shift means that the phase of the 5 day W1 PW in the temperature averaged over the height range of 81 to 87 km minus that in IWC. The negative phase shift means that the maximum (also the minimum) of W1 PW in the temperature occurs later than that of in the IWC. The x axis labels the DFS in the NPR and SPR. The years are labeled in each panel.

the downward progressing 5 day PWs should be related to the similar time-height distribution of eastward jet in the SPR as the regions of baroclinic/barotropic instability shifts downward. By contrast, neither the peak of zonal wind nor the 5 day PWs in the NPR shift downward with time.

In the upper mesosphere (above  $\sim 75$  km), 5 day PWs with different modes exhibit similar annual and semiannual variations in both the NPR and SPR, although their relative strengths vary (Figure 4). The W1 5 day PW in the NPR is stronger than in the SPR, especially at the height around 90 km. The 5 day PWs of the other modes (E1–E3, W0, W2, and W3) are stronger in the SPR than in the NPR. Since the W1 5 day PW is the strongest one in the summer upper mesosphere and is more closely related to the PMC [Merkel *et al.*, 2003, 2008, 2009; von Savigny *et al.*, 2007; Eckermann *et al.*, 2009; Nielsen *et al.*, 2010], we will focus on the relationships of the W1 5 day PWs in temperature and IWC in the next section.

#### 4. Phase Shift of the W1 5 Day PWs in the Temperature and IWC

Figure 2 has illustrated that the IWC is maximized when the temperature is minimized. These observations support the findings of previous studies on the relationships between temperature and PWCs derived from different satellite observations and data assimilation models [Merkel *et al.*, 2003, 2008, 2009; von Savigny *et al.*, 2007; Eckermann *et al.*, 2009; Hervig *et al.*, 2009b, 2013; Nielsen *et al.*, 2010]. An important finding in previous studies was a phase shift of 5 h or 10 h between the W1 5 day PWs in PMC brightness and temperature when PMC brightness is prominent. It should be noted that previous results often used PMC brightness and temperature that were separated in time and/or space. Data from different air columns may introduce uncertainty in the examination of the phase shift of W1 5 day PWs in PMC brightness and temperature. This shortcoming can be overcome through the use of the SOFIE instrument, which measures temperature and IWC simultaneously for the same air column.

##### 4.1. General Features of the Phase Shift

In extracting the 5 day PWs in temperature, we move the LS fitting window forward by 1 day. Thus, the temporal resolution of 5 day PWs in temperature is 1 day in section 3. To get a more precise phase relationship of the W1 5 day PWs in temperature and IWC, we move the LS fitting window forward by 1/15 day (~1.6 h, this is the time interval of the two continuous profiles from SOFIE observation). Consequently, the LS fitting is then performed within a sliding window of 120 h (5 day) with a 118.4 h overlap. Figure 5 shows the temporal evolution of the W1 5 day PWs in temperature and IWC at 120°E in summer from 2007 to 2014.

From Figure 5, we find that the W1 5 day PWs in temperature and IWC are almost antiphase (180° out of phase) at times when their amplitudes are substantial. The relatively stronger W1 5 day PW in the 32 to 50 DFS (e.g., early August) of 2007 has been reported in previous studies. The amplitude of the W1 5 day PW in temperature is less than 2 K during the main PMC seasons (June and July) and becomes stronger in the early August. This is in agreement with previous independent observations and model studies [Merkel *et al.*, 2009; Benze *et al.*, 2009; Eckermann *et al.*, 2009; Nielsen *et al.*, 2010]. In other years, relatively stronger W1 5 day PWs in temperature with an almost anticorrelation with those in IWC were found. By contrast, the phase relationship has been found to be very complex when the 5 day wave amplitudes of IWC and temperature are small (e.g., in the NPR: 0–30 DFS of 2007; entire summer of 2008; 20–40 DFS of 2009; –5–35 DFS of 2010; and in the SPR: 25–40 DFS of 2010–2011, 2011–2012, 2012–2013, 2013–2014, etc.). These results are consistent with previous findings of the 10 h or 5 h phase shift when the W1 5 day PWs are substantial and a very mixed phase shift during weak W1 5 day PWs [Merkel *et al.*, 2003, 2008, 2009; von Savigny *et al.*, 2007; Nielsen *et al.*, 2010].

To more accurately quantify the phase relationship between the W1 5 day PWs in IWC and temperature, Figure 6 shows the phase shift of the W1 5 day PWs in IWC and temperature when their correlation coefficient (CC) is minimized. We note that the minimum CC is achieved after varying the phase shift of W1 5 day PWs in temperature and IWC within a window of 15 day. Then we move the window forward by 1/15 day to get the time series of minimum CC in each PMC season. The minimum CC and the corresponding phase shift in one window may be different from those in another window. Thus, the phase shift shown in Figure 6 means that the time difference between the times at which the minimum (maximum) of temperature occurs and the times at which the maximum (minimum) IWC occurs. The magnitude of the negative CC represents the degree of anticorrelation between IWC and temperature. The negative CC indicates that the minimum temperature W1 5 day PW corresponds to the maximum IWC W1 5 day PW. Figure 6 shows that the phase shift varies from –15 h to 10 h in the NPR and from –20 h to 20 h in the SPR. Specifically, in the NPR, the phase shift varies from –5 h to 5 h with a CC of less than –0.8 in the early summer (from –20 to –5 DFS) of 2007. In the late summer (from 30 to 50 DFS) of 2007, the phase shift varies from –10 h to 0 h. In the SPR, the phase shift is about 0 h during most days in the summer of 2007–2008. The phase shift varies from –10 h to 10 h with a CC of less than –0.8 during the time interval of –30–30 DFS in 2008–2009 in the SPR. The phase shift is about –10 h during the time interval of –20 to –5 DFS in 2011–2012 in the SPR. These analyses indicate that the phase shift is not a simple value (e.g., 10 h or 5 h) as reported in previous studies [Merkel *et al.*, 2003, 2008, 2009; von Savigny *et al.*, 2007; Nielsen *et al.*, 2010]. In fact, the analyses of the 14 PMC seasons show that the phase shift exhibits day-to-day and year-to-year variations and interhemispheric asymmetry. Thus, it is necessary to

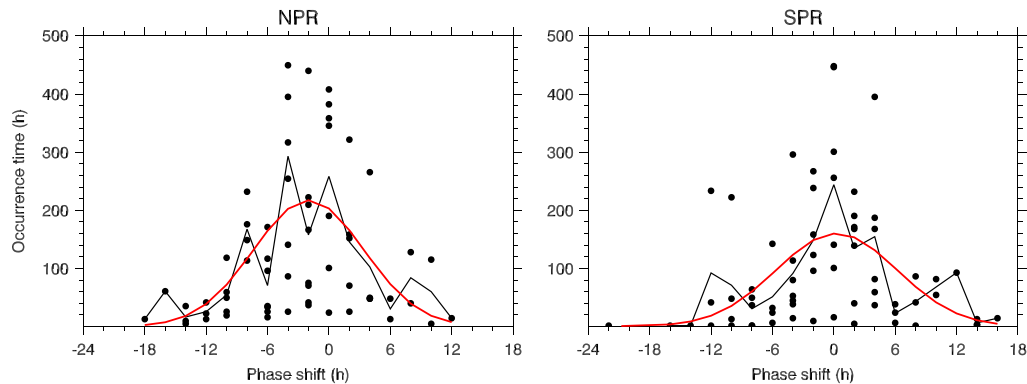


**Figure 7.** The occurrence time distribution (black dots) with respect to the phase shift in the (a) NPR and (b) SPR from 2007 to 2014. The occurrence time shown here under the condition when the correlation coefficient of W1 5 day PWs in temperature and IWC is less than  $-0.8$ . The black line is the mean occurrence time averaged from 2007 to 2014. The red line is the result of a Gaussian distribution fitting on the mean occurrence time.

characterize the phase shift in a statistical manner. It should be noted that the negative phase shift means that the maximum (also the minimum) of W1 PW in the temperature occurs later than that in the IWC. Because minimum temperature is favorable for the formation of PMC, thus, the temperature minimum should occur earlier than the IWC maximum. The phase shift should be positive. However, PMC formation depends on many factors, such as temperature, water vapor, and nucleation nuclei. PWs that perturb PMC variation will also perturb water vapor and nucleation nuclei. The maximum in water vapor and nucleation nuclei may not coincide with the coldest temperature. Moreover, the maximum in PMC may be reached before the minimum temperature due to the exhausted water vapor. These are possible reasons for the negative phase shift suggested in previous studies [Merkel *et al.*, 2003, 2008, 2009; von Savigny *et al.*, 2007; Nielsen *et al.*, 2010].

#### 4.2. Statistics of the Phase Shift

To quantify the phase shift between the W1 5 day PWs in IWC and temperature, we calculate the occurrence time distribution with respect to the phase shift when the CC is less than  $-0.8$ . Here the occurrence time with respect to the phase shift is defined as the sum of the time intervals during which they have the same phase shift. Figure 7 shows the occurrence time (black dots) with respect to the phase shift in the NPR and SPR from 2007 to 2014. The black lines are the mean occurrence time averaged over the 2007–2014 period. It can be seen that the phase shift varies from  $-18$  h to  $12$  h in the NPR and from  $-20$  h to  $16$  h in the SPR. The occurrence time distribution with respect to the phase shift was fitted with a Gaussian distribution

$$y_{fit} = a \exp \left[ -\left( \frac{t - t_0}{2\sigma_t} \right)^2 \right]. \quad (3)$$

Here  $t_0$  and  $\sigma_t$  are the mean and the standard deviation of phase shift, respectively. The fitted Gaussian distributions are shown as red lines in Figure 7. Our fitting results are  $a = 217.4$  h,  $t_0 = -2.0$  h, and  $\sigma_t = 3.8$  h in the NPR and  $a = 160.2$  h,  $t_0 = 0.3$  h, and  $\sigma_t = 4.2$  h in the SPR, respectively.

These results show that the mean phase shifts are  $-2.0$  h in the NPR and  $0.3$  h in the SPR, which indicate that the W1 5 day PW in IWC is nearly antiphased with the W1 5 day PW in temperature. This also indicates that the W1 5 day PW in temperature is the main driver of the W1 5 day PW in IWC and is consistent with earlier studies [e.g., Merkel *et al.*, 2003, 2008, 2009; von Savigny *et al.*, 2007; Nielsen *et al.*, 2010]. The standard deviations are  $3.8$  h in the NPR and  $4.2$  h in the SPR. This indicates that the variation of the phase shift is mainly within  $\sim 4$  h and varies in a relatively wider range in the SPR than in the NPR. This is a reasonable result because the formation of ice particles does not depend solely on the W1 5 day PW in temperature but depends on, and/or modulated by, gravity waves and mean temperature [Chandran *et al.*, 2010; Liu *et al.*, 2014b]. The

wave fluctuations with different periods can influence both the dynamics (e.g., convection, convergence, and divergence of the ice particles) and the microphysics of an ice particle [Jensen and Thomas, 1994]. Thus, the day-to-day and year-to-year variability of the mean temperature and various waves [Liu et al., 2014b] may be responsible for the variability of the phase shift of the W1 5 day PWs in temperature and IWC in the MLT region. Moreover, the formation of ice particles is also dependent on other factors, including the nucleation rate, number density of ice nuclei, and eddy diffusion [Rapp and Thomas, 2006; Nielsen et al., 2010]. Variations in any of these factors can influence the formation of ice and thus the phase shift of the W1 5 day PWs in temperature and IWC.

## 5. Summary and Conclusions

Using 8 years (2007–2014) of temperature profiles and IWC observed by the SOFIE instrument on board the AIM satellite, we analyzed 5 day PWs with zonal wave numbers ranging from  $-3$  to  $-1$  (eastward propagating modes, E3–E1),  $0$  (stationary mode, W0), and  $1$  to  $3$  (westward propagating modes, W1–W3). The 5 day PWs with different zonal wave numbers were extracted using the LS method. The extracted 5 day PWs in temperature cover the entire stratosphere and mesosphere (16–94 km) over Arctic and Antarctic. Then the climatologies of 5 day PWs were analyzed with respect to seasonal variations, the relative strength of different wave numbers and height dependence and interhemispheric asymmetry. The 5 day PWs in IWC were also extracted at the summer mesopause (81–87 km). Taking advantage of the simultaneous measurement of temperature and IWC, the phase relationships of the W1 5 day PWs in temperature and IWC were then analyzed.

The 5 day PWs in temperature with different wave numbers were shown to be stronger in winter, and the relative strengths of 5 day PWs were shown to be dependent on height and zonal wave numbers. In the winter stratosphere and lower mesosphere, the E1 5 day PW was stronger than in any other mode in both the NPR and SPR. However, in the upper mesosphere (above  $\sim 75$  km), the W1 5 day PWs in winter and summer were comparable. The stronger 5 day PWs in the winter polar region was likely generated from barotropic/baroclinic instability in the polar night jet and/or double-jet structure in the winter polar stratosphere. The W1 5 day PW in summer may be ducted from the winter hemisphere and/or generated in situ by baroclinic instability in the MLT region.

The 5 day PWs with propagation modes exhibited great interhemispheric asymmetry in the stratosphere and lower mesosphere. Moreover, the interhemispheric asymmetry was wave number and height dependent. In the upper mesosphere, the W1 5 day PW in the NPR was stronger than in the SPR. The 5 day PW peaks extended to lower altitudes with time in the SPR. This was consistent with the time-height distribution of eastward jet in the SPR and thus the regions of baroclinic/barotropic instability. However, the 5 day PWs and the eastward jet did not show this feature in the NPR.

The phase relationship between the W1 5 day PWs in temperature and IWC were analyzed based on this 8 year data, which cover 14 PMC seasons in total. We found that the phase shift of the W1 5 day PW in temperature relative to that in IWC varies in a wide range from  $-18$  h to  $12$  h and from  $-20$  h to  $16$  h in the NPR and SPR, respectively. However, the phase shift between the W1 5 day PWs in temperature and IWC had a mean value of  $-2.0$  h ( $0.3$  h) and a standard deviation of  $3.8$  h ( $4.2$  h) in the NPR (SPR). The mean phase shift of  $\sim 0$  h indicated that the W1 5 day PW in IWC is mainly dependent on the W1 5 day PW in temperature. The variation in the phase shift indicated that the formation of IWC is also influenced by other factors.

## Appendix A

The Monte Carlo method was used to calculate the confidence level of 5 day PWs in each window [Pardo-Igúzquiza and Rodríguez-Tovar, 2012]. This method is described briefly as follows. First, the LS fitting is applied to the original series, and a spectral amplitude ( $A_0$ ) is obtained. Then the LS fitting is applied to the random permuted series to get a spectral amplitude ( $A_i$ ). Here the permutation of time series is that a sequence of the original observations is randomly permuted and the original time locations are retained. Finally, the CL is calculated by dividing the total number of random tests

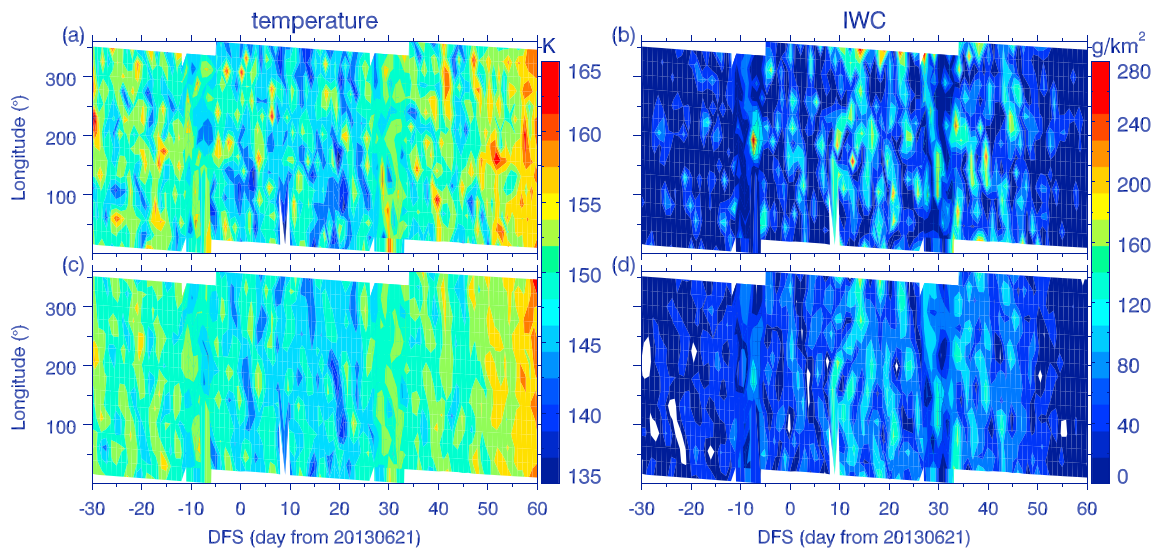


**Figure A1.** Hovmöller plots of the observed temperature averaged over the height range of (a) 81 to 87 km (b) and IWC and the LS fitted of 5 day PWs in (c) temperature and (d) IWC with zonal wave number from  $-3$  to  $3$  and with a 5 day window during the summer of 2003.

from the total number of random tests with  $A_0$  greater than or equal to  $A_i$ . A detailed description of this method can be found in *Pardo-Igúzquiza and Rodríguez-Tovar [2012]*. This method has been used by *Liu et al. [2014a]* to calculate the planetary wave type oscillations in the thermosphere winds. In a similar manner, 200 random tests were performed to calculate CL.

Increasing the window size reduces both the spectral uncertainty and the temporal resolution, but it also smoothens out some short-lived wave events [*Wu et al., 1995*]. Thus, a proper window size should be chosen so that the spectra have sufficient CL and temporal resolution. To get a proper window size, significance tests were performed on the observational data with three different window sizes: (1) a sliding 5 day window, (2) a sliding 10 day window, and (3) a sliding 15 day window. The sliding window was forwarded 1 day for these significance tests. The SOFIE/AIM instrument provides 15 temperature profiles and IWC data covering  $360^\circ$  in longitude each day. Figure A1 shows Hovmöller plots of the observed temperature averaged over the height range of 81 to 87 km (Figure A1a) and IWC (Figure A1b) around the summer solstice of 2013. These data are taken as an example to show the confidence level and the fitted 5 day PWs.

Figure A2 shows amplitudes and confidence level of the 5 day PWs with zonal wave numbers from  $-3$  to  $-1$  (eastward propagating modes, E3–E1), 0 (stationary mode, W0), and from 1 to 3 (westward propagating modes, W1–W3) obtained by performing the LS method with three different window sizes. Figure A2 illustrates that increasing the window size does not increase the CL significantly but does suppress wave amplitude. In the results from the three different window sizes, the CLs of W0 and W1 5 day PWs are higher than 60% during most of the observations. However, the confidence levels of 5 day PWs with other wave numbers are lower than 60% during most of the observations. For the 5 day PWs in temperature and IWC, both their amplitudes and CL decrease with the increasing wave numbers. This shows that the W0 and W1 5 day PWs are substantial both in temperature and IWC. This also supports the previous findings that the W1 5 day PW is prominent both in temperature and PMC [*Merkel et al., 2003, 2008, 2009; von Savigny et al., 2007; Nielsen et al., 2010*].

Since the 5 day window can capture the 5 day PWs with a statistically significant CL and high temporal resolution, we show in Figures A1c and A1d the fitted 5 day PWs in temperature and IWC with zonal wave numbers ranging from  $-3$  to  $3$  in a 5 day window, respectively. Comparisons between observations (Figures A1a and A1b) and the corresponding fitting results (Figures A1c and A1d) illustrate that the fitting results in a 5 day window can accurately capture the observational features. Thus, the 5 day window is used in our analysis.

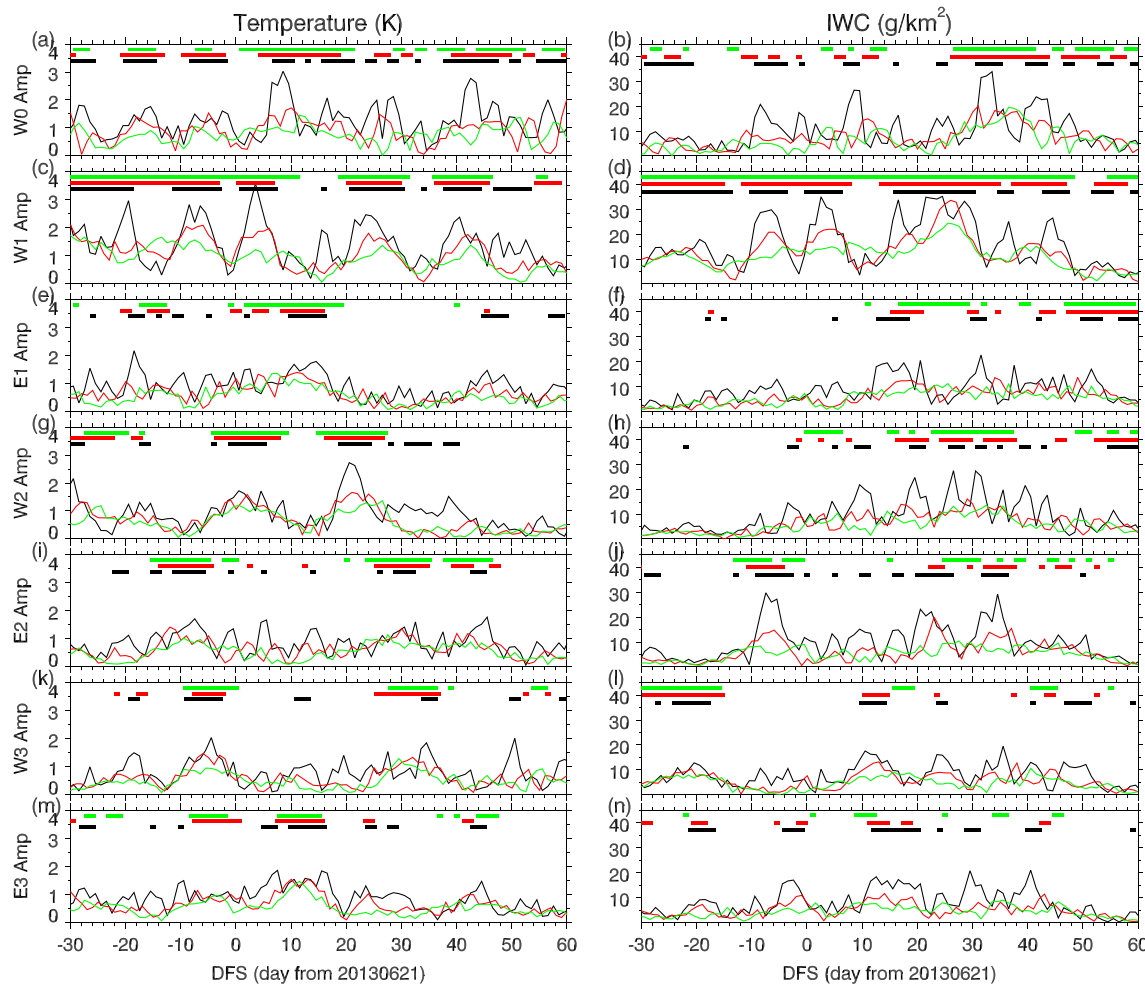


**Figure A2.** Amplitudes of the 5 day PWs with zonal wave numbers of (a and b) 0 (W0), (c and d) 1 (westward, W1), (e and f) –1 (eastward, E1), (g and h) 2 (westward, W2), (i and j)–2 (eastward, E2), (k and l) 3 (westward, W3), and (m and n) –3 (eastward, E3) extracted from the (left) temperature and (right) IWC shown in Figures A1a and A1b, respectively. The time intervals when the amplitude is significant at the 60% confidence level are shown as horizontal bars. The amplitude and CL are obtained by LS method in window sizes of 5 day, 10 day, and 15 day and are shown as black, red, and green, respectively.

#### Acknowledgments

We thank the efforts of the AIM SOFIE data (<ftp://ftp.gats-inc.com>) processing and science teams. This work was supported by the Chinese Academy of Sciences (KZZD-EW-01-2), the National Science Foundation of China (41374158, 41229001, and 41331069), and the National Important Basic Research Project (grant 2011CB811405), and Educational Commission of Henan Province of China (13A110547, and 2014GGJS-047). This work was also supported in part by the Specialized Research Fund and the Open Research Program of the State Key Laboratory of Space Weather.

#### References

- Allen, D. R., J. L. Stanford, L. S. Elson, E. F. Fishbein, L. Froidevaux, and J. W. Waters (1997), The 4 day wave as observed from the Upper Atmosphere Research Satellite Microwave Limb Sounder, *J. Atmos. Sci.*, 54, 420–434.
- Altadill, D., and E. M. Apostolov (2003), Time and scale size of planetary wave signatures in the ionospheric F region: Role of the geomagnetic activity and mesosphere/lower thermosphere winds, *J. Geophys. Res.*, 108(A11), 1403, doi:10.1029/2003JA010015.
- Bailey, S. M., B. Thurairajah, C. E. Randall, L. Holt, D. E. Siskind, V. L. Harvey, K. Venkataramani, M. E. Hervig, P. Rong, and J. M. Russell III (2014), A multitracer analysis of thermosphere to stratosphere descent triggered by the 2013 Stratospheric Sudden Warming, *Geophys. Res. Lett.*, 41, 5216–5222, doi:10.1002/2014GL059860.
- Benze, S., C. E. Randall, M. T. DeLand, G. E. Thomas, D. W. Rusch, S. M. Bailey, J. M. Russell III, W. E. McClintock, A. W. Merkel, and C. Jeppesen (2009), Comparison of polar mesospheric cloud measurements from the cloud imaging and particle size experiment and the solar backscatter ultraviolet instrument in 2007, *J. Atmos. Sol. Terr. Phys.*, 71, 365–372, doi:10.1016/j.jastp.2008.07.014.
- Chandran, A., D. W. Rusch, A. W. Merkel, S. E. Palo, G. E. Thomas, M. J. Taylor, S. M. Bailey, and J. M. Russell III (2010), Polar mesospheric cloud structures observed from the cloud imaging and particle size experiment on the Aeronomy of Ice in the Mesosphere spacecraft: Atmospheric gravity waves as drivers for longitudinal variability in polar mesospheric cloud occurrence, *J. Geophys. Res.*, 115, D13102, doi:10.1029/2009JD013185.
- Charney, J. G., and P. G. Drazin (1961), Propagation of planetary-scale disturbances from the lower into the upper atmosphere, *J. Geophys. Res.*, 66(1), 83–109, doi:10.1029/JZ066i001p00083.
- Clark, R. R., M. D. Burridge, S. J. Franke, A. H. Manson, C. E. Meek, N. J. Mitchell, and H. G. Muller (2002), Observations of 7 day planetary waves with MLT radars and the UARS-HRDI instrument, *J. Atmos. Sol. Terr. Phys.*, 64, 1217–1228, doi:10.1016/S1364-6826(02)00070-6.
- Coy, L., I. Stajner, A. M. Dasilva, J. Joiner, R. B. Rood, S. Pawson, and S. J. Lin (2003), High-frequency planetary waves in the polar middle atmosphere as seen in a data assimilation system, *J. Atmos. Sci.*, 60, 2975–2992.
- Day, K. A., and N. J. Mitchell (2010), The 5 day wave in the Arctic and Antarctic mesosphere and lower thermosphere, *J. Geophys. Res.*, 115, D01109, doi:10.1029/2009JD012545.

- Eckermann, S. D., K. W. Hoppel, L. Coy, J. P. McCormack, D. E. Siskind, K. Nielsen, A. Kochenash, M. H. Stevens, C. R. Englert, and M. E. Hervig (2009), High-altitude data assimilation system experiments for the northern summer mesosphere season of 2007, *J. Atmos. Sol. Terr. Phys.*, **71**, 531–551, doi:10.1016/j.jastp.2008.09.036.
- Forbes, J. M. (1995), Tidal and planetary waves, in *The Upper and Lower Thermosphere: A Review of Experiment and Theory*, *Geophys. Monogr. Ser.*, vol. 87, edited by R. M. Johnson and T. L. Killeen, pp. 67–87, AGU, Washington, D. C.
- Garcia, R. R., R. Lieberman, J. M. Russell III, and M. G. Mlynczak (2005), Large-scale wave in the mesosphere and lower thermosphere observed by SABER, *J. Atmos. Sci.*, **62**, 4384–4399.
- Gordley, L. L., et al. (2009), The solar occultation for ice experiment, *J. Atmos. Sol. Terr. Phys.*, **71**, 300–315, doi:10.1016/j.jastp.2008.07.012.
- Hervig, M. E., R. E. Thompson, M. McHugh, L. L. Gordley, J. M. Russell, and M. E. Summers (2001), First confirmation that water ice is the primary component of polar mesospheric clouds, *Geophys. Res. Lett.*, **28**, 971–974, doi:10.1029/2000GL012104.
- Hervig, M. E., L. L. Gordley, M. Stevens, J. M. Russell, S. Bailey, and G. Baumgarten (2009a), Interpretation of SOFIE PMC measurements: Cloud identification and derivation of mass density, particle shape, and particle size, *J. Atmos. Sol. Terr. Phys.*, **71**, 316–330, doi:10.1016/j.jastp.2008.07.009.
- Hervig, M. E., M. H. Stevens, L. L. Gordley, L. E. Deaver, J. M. Russell III, and S. M. Bailey (2009b), Relationships between polar mesospheric clouds, temperature, and water vapor from Solar Occultation for Ice Experiment (SOFIE) observations, *J. Geophys. Res.*, **114**, D20203, doi:10.1029/2009JD012302.
- Hervig, M. E., D. E. Siskind, M. H. Stevens, and L. E. Deaver (2013), Interhemispheric comparison of PMCs and their environment from SOFIE observations, *J. Atmos. Sol. Terr. Phys.*, **104**, 285–298, doi:10.1016/j.jastp.2012.10.013.
- Jensen, E. J., and G. E. Thomas (1994), Numerical simulations of the effects of gravity waves on noctilucent clouds, *J. Geophys. Res.*, **99**, 3421–3430, doi:10.1029/93JD01736.
- Jiang, G., et al. (2008), A case study of the mesospheric 6.5 day wave observed by radar systems, *J. Geophys. Res.*, **113**, D16111, doi:10.1029/2008JD009907.
- Kasahara, A. (1976), Normal modes of ultralong waves, *Mon. Weather Rev.*, **104**, 669–690.
- Kirkwood, S., and K. Stebel (2003), Influence of planetary waves on noctilucent cloud occurrence over NW Europe, *J. Geophys. Res.*, **108**(D8), 8440, doi:10.1029/2002JD002356.
- Kovalam, S., R. A. Vincent, I. M. Reid, T. Tsuda, T. Nakamura, K. Ohnishi, A. Nuryanto, and H. Wiryosumarto (1999), Longitudinal variations in planetary wave activity in the equatorial mesosphere, *Earth Planets Space*, **51**, 665–674.
- Lawrence, B. N., and W. J. Randel (1996), Variability in the mesosphere observed by the Nimbus 6 pressure modulator radiometer, *J. Geophys. Res.*, **101**(D18), 23,475–23,489, doi:10.1029/96JD01652.
- Lieberman, R. S., D. M. Riggan, S. J. Franke, A. H. Manson, C. Meek, T. Nakamura, T. Tsuda, R. A. Vincent, and I. Reid (2003), The 6.5 day wave in the mesosphere and lower thermosphere: Evidence for baroclinic/barotropic instability, *J. Geophys. Res.*, **108**(D20), 4640, doi:10.1029/2002JD003349.
- Liu, H.-L., E. R. Talaat, R. G. Roble, R. S. Lieberman, D. M. Riggan, and J.-H. Yee (2004), The 6.5 day wave and its seasonal variability in the middle and upper atmosphere, *J. Geophys. Res.*, **109**, D21112, doi:10.1029/2004JD004795.
- Liu, H.-L., W. Wang, A. D. Richmond, and R. G. Roble (2010), Ionospheric variability due to planetary waves and tides for solar minimum conditions, *J. Geophys. Res.*, **115**, A00G01, doi:10.1029/2009JA015188.
- Liu, X., J. Xu, S. Zhang, G. Jiang, Q. Zhou, W. Yuan, J. Noto, and R. Kerr (2014a), Thermospheric planetary wave-type oscillations observed by FPIs over Xinglong and Millstone Hill, *J. Geophys. Res. Space Physics*, **119**, 6891–6901, doi:10.1002/2014JA020043.
- Liu, X., J. Yue, J. Xu, L. Wang, W. Yuan, J. M. Russell III, and M. E. Hervig (2014b), Gravity wave variations in the polar stratosphere and mesosphere from SOFIE/ AIM temperature observations, *J. Geophys. Res. Atmos.*, **119**, 7368–7381, doi:10.1002/2013JD021439.
- Lomb, N. R. (1976), Least-square frequency analysis of unequally spaced data, *Astrophys. Space Sci.*, **39**, 447–462.
- Lu, X., X. Chu, T. Fuller-Rowell, L. Chang, W. Fong, and Z. Yu (2013), Eastward propagating planetary waves with periods of 1–5 days in the winter Antarctic stratosphere as revealed by MERRA and lidar, *J. Geophys. Res. Atmos.*, **118**, 9565–9578, doi:10.1002/jgrd.50717.
- Luo, Y., et al. (2002), The 16 day planetary waves: Multi-MF radar observations from the arctic to equator and comparisons with the HRDI measurements and the GSWM modelling results, *Ann. Geophys.*, **20**, 691–709.
- Madden, R. A. (1979), Observations of large-scale traveling Rossby waves, *Rev. Geophys.*, **17**, 1935–1949, doi:10.1029/RG017i008p01935.
- Manney, G. L., and W. J. Randel (1993), Instability at the winter stratopause: A mechanism for the 4 day wave, *J. Atmos. Sci.*, **50**, 3928–3938.
- Marshall, B. T., L. E. Deaver, R. E. Thompson, L. L. Gordley, M. J. McHugh, M. E. Hervig, and J. M. Russell III (2011), Retrieval of temperature and pressure using broadband solar occultation: SOFIE approach and results, *Atmos. Meas. Tech.*, **4**, 893–907, doi:10.5194/amt-4-893-2011.
- Merkel, A. W., G. E. Thomas, S. E. Palo, and S. M. Bailey (2003), Observations of the 5 day planetary wave in PMC measurements from the Student Nitric Oxide Explorer Satellite, *Geophys. Res. Lett.*, **30**(4), 1196, doi:10.1029/2002GL016524.
- Merkel, A. W., R. R. Garcia, S. M. Bailey, and J. M. Russell III (2008), Observational studies of planetary waves in PMCs and mesospheric temperature measured by SNOE and SABER, *J. Geophys. Res.*, **113**, D14202, doi:10.1029/2007JD009396.
- Merkel, A. W., D. W. Rusch, S. E. Palo, J. M. Russell III, and S. M. Bailey (2009), Mesospheric planetary wave activity inferred from AIM/CIPS and TIMED/SABER for the northern summer 2007 PMC season, *J. Atmos. Sol. Terr. Phys.*, **71**, 381–391, doi:10.1016/j.jastp.2008.12.001.
- Nielsen, K., D. E. Siskind, S. D. Eckermann, K. W. Hoppel, L. Coy, J. P. McCormack, S. Benze, C. E. Randall, and M. E. Hervig (2010), Seasonal variation of the quasi 5 day planetary wave: Causes and consequences for polar mesospheric cloud variability in 2007, *J. Geophys. Res.*, **115**, D18111, doi:10.1029/2009JD012676.
- Palo, S. E., J. M. Forbes, X. Zhang, J. M. Russell III, C. J. Mertens, M. G. Mlynczak, G. B. Burns, P. J. Espy, and T. D. Kawahara (2005), Planetary wave coupling from the stratosphere to the thermosphere during the 2002 Southern Hemisphere pre-stratwarm period, *Geophys. Res. Lett.*, **32**, L23809, doi:10.1029/2005GL024298.
- Pancheva, D. V., and N. J. Mitchell (2004), Planetary waves and variability of the semidiurnal tide in the mesosphere and lower thermosphere over Esrange (68°N, 21°E) during winter, *J. Geophys. Res.*, **109**, A08307, doi:10.1029/2004JA010433.
- Pancheva, D., and P. Mukhtarov (2011), Atmospheric tides and planetary waves: Recent progress based on SABER/TIMED temperature measurements (2002–2007), in *Aeronomy of the Earth's Atmosphere and Ionosphere*, *IAGA Spec. Sopron Book Ser.*, vol. 2, edited by M. A. Abdu, D. Pancheva, and A. Bhattacharyya, pp. 19–56, Springer, New York, doi:10.1007/978-94-007-0326-1\_2.
- Pancheva, D., P. Mukhtarov, B. Andonov, and J. M. Forbes (2010), Global distribution and climatological features of the 5–6 day planetary waves seen in the SABER/TIMED temperatures (2002–2007), *J. Atmos. Sol. Terr. Phys.*, **72**(1), 26–37, doi:10.1016/j.jastp.2009.10.005.
- Pardo-Igúzquiza, E., and F. J. Rodríguez-Tovar (2012), Spectral and cross-spectral analysis of uneven time series with the smoothed Lomb–Scargle periodogram and Monte Carlo evaluation of statistical significance, *Comput. Geosci.*, **49**, 207–216.
- Pogoreltsev, A. I., A. A. Vlasov, K. Fröhlich, and C. Jacobi (2007), Planetary waves in coupling the lower and upper atmosphere, *J. Atmos. Sol. Terr. Phys.*, **69**, 2083–2101.

- Prata, A. J. (1989), Observations of the 5 day wave in the stratosphere and mesosphere, *J. Atmos. Sci.*, 46(15), 2473–2477.
- Rapp, M., and G. E. Thomas (2006), Modeling the microphysics of mesospheric ice particles: Assessment of current capabilities and basic sensitivities, *J. Atmos. Sol. Terr. Phys.*, 68, 715–744, doi:10.1016/j.jastp.2005.10.015.
- Riggin, D. M., et al. (2006), Observations of the 5 day wave in the mesosphere and lower thermosphere, *J. Atmos. Sol. Terr. Phys.*, 68, 323–339, doi:10.1016/j.jastp.2005.05.010.
- Russell, J. M., III et al. (2009), The Aeronomy of Ice in the Mesosphere (AIM) mission: Overview and early science results, *J. Atmos. Sol. Terr. Phys.*, 71, 289–299, doi:10.1016/j.jastp.2008.08.011.
- Salby, M. L. (1981), Rossby normal modes in nonuniform background configurations. Part I: Simple fields, *J. Atmos. Sci.*, 38, 1803–1826.
- Shepherd, G. G., et al. (2012), The Wind Imaging Interferometer (WINDII) on the Upper Atmosphere Research Satellite: A 20 year perspective, *Rev. Geophys.*, 50, RG2007, doi:10.1029/2012RG000390.
- Stevens, M. H., L. E. Deaver, M. E. Hervig, J. M. Russell III, D. E. Siskind, P. E. Sheese, E. J. Llewellyn, R. L. Gattinger, J. Höffner, and B. T. Marshall (2012), Validation of upper mesospheric and lower thermospheric temperatures measured by the Solar Occultation For Ice Experiment, *J. Geophys. Res.*, 117, D16304, doi:10.1029/2012JD017689.
- Thomas, G. E. (1996), Is the polar mesosphere the miner's canary of global change?, *Adv. Space Res.*, 18, 149–158.
- Thurairajah, B., S. M. Bailey, C. Y. Cullens, M. E. Hervig, and J. M. Russell III (2014), Gravity wave activity during recent stratospheric sudden warming events from SOFIE temperature measurements, *J. Geophys. Res. Atmos.*, 119, 8091–8103, doi:10.1002/2014JD021763.
- von Savigny, C., C. Roberts, H. Bovensmann, J. P. Burrows, and M. Schwartz (2007), Satellite observations of the quasi 5 day wave in noctilucent clouds and mesopause temperatures, *Geophys. Res. Lett.*, 34, L24808, doi:10.1029/2007GL030987.
- Watanabe, S., Y. Tomikawa, K. Sato, Y. Kawatani, K. Miyazaki, and M. Takahashi (2009), Simulation of the eastward 4 day wave in the Antarctic winter mesosphere using a gravity wave resolving general circulation model, *J. Geophys. Res.*, 114, D16111, doi:10.1029/2008JD011636.
- Wu, D. L., P. B. Hays, and W. R. Skinner (1994), Observations of the 5 day wave in the mesosphere and lower thermosphere, *Geophys. Res. Lett.*, 21(24), 2733–2736, doi:10.1029/94GL02660.
- Wu, D. L., P. B. Hays, and W. R. Skinner (1995), A least squares method for spectral analysis of space-time series, *J. Atmos. Sci.*, 52(20), 3501–3511.
- Yue, J., W. Wang, A. D. Richmond, and H.-L. Liu (2012), Quasi-two day wave coupling of the mesosphere and lower thermosphere-ionosphere in the TIME-GCM: Two-day oscillations in the ionosphere, *J. Geophys. Res.*, 117, A07305, doi:10.1029/2012JA017815.